

# Collective dynamics of complex plasma bilayers

P Hartmann<sup>1,2</sup>, Z Donkó<sup>1,2</sup>, G J Kalman<sup>2</sup>, S Kyrkos<sup>3</sup>, K I Golden<sup>4</sup>, and M Rosenberg<sup>5</sup>

<sup>1</sup>*Research Institute for Solid State Physics and Optics of the Hungarian Academy of Sciences, H-1525 Budapest, P. O. Box 49, Hungary*

<sup>2</sup>*Department of Physics, Boston College, 140 Commonwealth Ave, Chestnut Hill, MA, 02467, USA*

<sup>3</sup>*Department of Chemistry & Physics, Le Moyne College, 1419 Salt Springs Road, Syracuse, NY 13214, USA*

<sup>4</sup>*Department of Mathematics and Statistics, College of Engineering and Mathematical Sciences, University of Vermont, Burlington, VT 05401-1455, USA and*

<sup>5</sup>*Department of Electrical and Computer Engineering, University of California San Diego, La Jolla, CA, 92093, USA*

A classical dusty plasma experiment was performed using two different dust grain sizes to form a strongly coupled asymmetric bilayer (two closely spaced interacting monolayers) of two species of charged dust particles. The observation and analysis of the thermally excited particle oscillations revealed the collective mode structure and wave dispersion in this system; in particular the existence of the theoretically predicted  $k = 0$  energy (frequency) gap was verified. Equilibrium molecular dynamics simulations were performed to emulate the experiment, assuming Yukawa type interparticle interaction. The simulations and analytic calculations based both on lattice summation and on the QLCA approach are in good agreement with the experimental findings and help identifying and characterizing the observed phenomena.

Particle bilayers (parallel planes occupied by interacting particles and separated by a distance comparable to the interparticle distance within the layers) can be viewed as an intermediate stage between two-dimensional (2D) and three-dimensional (3D) systems. It is the interplay of the 3D interaction and the 2D dynamics that creates the rich new physics predicted and observed in interacting bilayers that makes these systems interesting in their own right. At the same time, bilayer configurations are also ubiquitous in widely different physical systems. Of special importance are those of charged particles (with like charges: unipolar bilayer, or with opposite charges: bipolar bilayer). Examples are semiconductor heterostructures [1], cryogenic traps [2], overdamped system of lipid membranes [3], interfacial superconductors [4], etc.

From the theoretical point of view, during the past three decades unipolar layered systems were studied in the weak coupling limit by means of analytic calculations [5, 6] and in the strongly coupled regime by semi-analytic lattice calculations [7], approximate liquid state calculations [8] and computer simulations [9, 10, 11, 12, 13]. More recently, bipolar (electron–hole) bilayers have been the focus of intense computer simulation efforts, both in the classical [14, 15, 16] and in the quantum regimes [17, 18], where features such as structural phase transitions, bound dipole formation [19], etc. were detected.

Very recently a seminal observation by Hyde *et.al.* [20] has led to the realization that strongly coupled unipolar bilayers can be created in laboratory complex (dusty) plasma environments. This can be accomplished by using a mixture of two differently sized grains: in view of their necessarily different charge to mass ( $Z/m$ ) ratios, the two species would settle at different equilibrium heights in the plasma sheath, as governed by the local balance of gravitational and electric forces. Thus this

novel type of bilayer would be, in contrast to most of the previously observed ones, a binary bilayer with hitherto unexplored features. Its structural properties were already reported in [20]. Subsequent computer simulations predicting collective excitations (wave propagation) and their dispersion were carried out in recent years both for Coulomb and Yukawa type isotropic interactions [21, 22].

In this Letter we report on the experimental investigation of the collective dynamical properties of a binary dusty plasma system. Our results constitute the first observation of the mode spectrum of a strongly coupled (liquid or solid) bilayer. Earlier results [23] were restricted to the weakly coupled state, where all collective modes exhibit an acoustic behavior. We confirm the predicted [7, 8] benchmark of the strongly coupled mode structure, the development of optic modes with a wave-number  $k = 0$  “energy (frequency) gap”.

Our dusty plasma experiments have been carried out in a custom designed vacuum chamber with an inner diameter of 25 cm and height of 18 cm. The lower, powered, 18 cm diameter, flat, horizontal, stainless steel electrode faces the upper, ring shaped, grounded aluminum electrode with an inner diameter of 15 cm at a height of 13 cm. Experiments have been performed in (4.6 purity) argon gas discharge at a pressure  $p = 0.8 \pm 0.05$  Pa, in a steady gas flow of  $\sim 0.01$  sccm, with 13.56 MHz radio frequency excitation of  $\sim 5$  W power. In the experiment melamine-formaldehyde micro-spheres with diameters  $d_1 = 3.63 \pm 0.06 \mu\text{m}$  and  $d_2 = 4.38 \pm 0.06 \mu\text{m}$  are used. For illumination we apply a 200 mW, 532 nm dpss-laser. Our CCD camera has a resolution of 1.4 Megapixels and runs at 29.54 frames per second acquisition rate. Particle masses are:  $m_1 = 3.8 \cdot 10^{-14}$  kg and  $m_2 = 6.6 \cdot 10^{-14}$  kg.

During the evaluation of the raw images (typically over 60000 per experiment) identification and position mea-

surement of the particles is performed using the method described in [24]. The identification of the light and heavy (smaller and larger) particles is based on their scattered intensities, which is in this size domain proportional to the square of the diameter. After tracing the particles motion from frame to frame we obtain the positions and velocities of each particle as a function of time. The layer separation was measured by simply rotating the camera and illuminating setup and taking images through the side window. After calibrating with a size standard we find the following average structural parameters: number of particles:  $N_1 = 682$ ,  $N_2 = 636$ ; the Wigner-Seitz radius calculated from the total number of the observed particles ( $N$ ) and the area ( $A$ ) of the field of view:  $a = \sqrt{A/\pi N} = 0.243$  mm (in the following distances appear normalized to  $a$ ); layer separation  $\bar{d} = d/a = 0.43$ .

Based on the particle positions the  $g(r)$  pair distribution function is obtained and compared to molecular-dynamics (MD) simulation results, (which was carried out by using the same input parameters as in the experiment), as shown in Fig. 1. Comparing experiment and simulation, one can conclude, that both capture qualitatively identical features: order, shape and position of the peaks agree satisfactorily. Differences in the amplitude and decay rate are due to friction and density gradients due to the finite and confined nature of the experimental system. In the simulation infinite system size (periodic boundaries) and no friction are assumed. Also, the layer assignment procedure during the data processing has some degree of uncertainty. Peak positions are consistent with the underlying hexagonal lattice structure, in agreement with theoretical results in [7, 12].

Visual observation of the recorded images confirms that most of the system is in a hexagonal configuration, sometimes small domains with rhombic and square unit cells were also found. Although the ground state configuration for a bilayer is a regular staggered rectangular lattice, a large degree of substitutional disorder [25], due to the small inter-layer separation and the finite temperature, was observed, as shown in the particle snapshots in Fig. 1.

In the MD simulation Yukawa type pair-interaction  $\Phi_{ij} = (e^2 Z_i Z_j / 4\pi\epsilon_0) \exp[-r_{ij}/\lambda_D] / r_{ij}$ , where  $r_{ij}$  is the three-dimensional distance between particles  $i$  and  $j$ , is assumed using  $\sim 4000$  particles with periodic boundary conditions. Since the interlayer separation is of the order of  $1/4\lambda_D$ , the attractive force between grains in the two layers due to ion focusing or wakefield effects are assumed to be small, since these effects occur generally at larger separations (see e.g. [26]). The neglect of such attractive forces is further bolstered by the experimental observation that the grains in the two layers do not form strings, but rather assume a staggered structure. Particle densities, masses and layer separation are taken from the experiment,  $\kappa = a/\lambda_D = 0.5$  and  $Z_1 = 2550$ ,

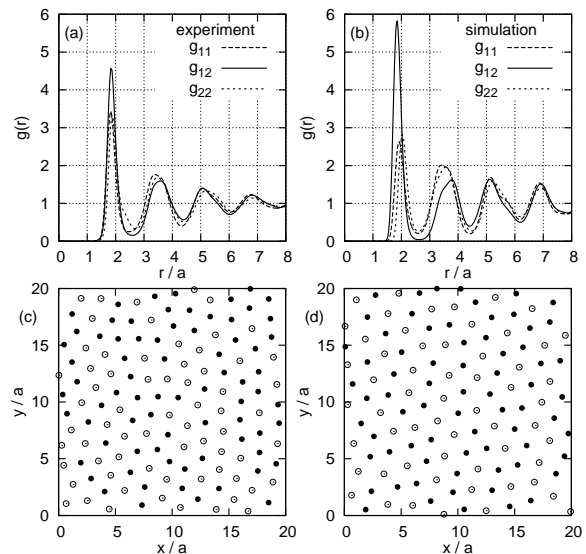


FIG. 1: Pair-distribution functions and particle snapshots obtained from the experiment (a,c) and the MD simulation (b,d). Indexes and symbol types label the layers [open: layer 1, filled: layer 2].

$Z_2 = (d_2/d_1)Z_1 \approx 3080$  are further assumed; this parameter set was found in lattice calculations to best reproduce experimental dispersions.

In the experiment we observe a pressure jump of about 38% when switching on the discharge. Taking into account the active and the total volume of the vacuum system, this results in an  $\approx 85\%$  average temperature increase in the discharge region, resulting in  $T_p \approx 550K$ . Measuring the dust particle velocities gives the direct kinetic energy, resulting in  $T_{v1} \approx 400K$  and  $T_{v2} \approx 500K$  for the two layers, and the Coulomb coupling parameters [defined as  $\Gamma_m = (e^2/4\pi\epsilon_0)(Z_m^2/k_B T_m a_m)$ ]:  $\Gamma_1 \approx 800$  and  $\Gamma_2 \approx 900$ . To obtain dynamical information on the system's collective excitations we use the method based on the Fourier transform of the microscopic density and current fluctuations, already successfully applied in MD simulations, see e.g. [11, 27]. Knowing the particle positions vs. time, first we calculate the microscopic densities, as well as longitudinal and transverse currents:  $\rho^{(m)}(\mathbf{k}, t) = \sum_j \exp(-i\mathbf{k} \cdot \mathbf{r}_j)$ ,  $\lambda^{(m)}(\mathbf{k}, t) = \sum_j v_{j,\parallel} \exp(-i\mathbf{k} \cdot \mathbf{r}_j)$ ,  $\tau^{(m)}(\mathbf{k}, t) = \sum_j v_{j,\perp} \exp(-i\mathbf{k} \cdot \mathbf{r}_j)$  for the two layers ( $m = 1, 2$ ). From the Fourier transforms of  $\rho(\mathbf{k}, t) \rightarrow \rho(\mathbf{k}, \omega)$ ,  $\lambda \rightarrow \lambda(\mathbf{k}, \omega)$ , and  $\tau \rightarrow \tau(\mathbf{k}, \omega)$  one can calculate the power spectra, e.g.  $S_{m,n}(\mathbf{k}, \omega) \propto \langle \rho^{(m)}(-\mathbf{k}, -\omega) \rho^{(n)}(\mathbf{k}, \omega) \rangle$ , averaging is over the time-slices available. In the present case of an asymmetric bilayer the labeling of the modes is not possible in a simple way, as it is for symmetric bilayers [11], where the two “+” and “-” polarizations clearly separate and correspond to in-, and out-of-phase oscillations. Therefore, in the following we do not label the modes, only indicate in which spectra they appear as peaks. For an analysis of

the mode structure one has to examine the spectra individually and identify the peak positions. Sample spectra are shown in Fig. 2 to illustrate the fundamental features in more detail. Plotted are results of the bilayer experiment and of the MD simulation; also to serve as reference standard, results of a separately performed single layer experiment carried out in the same experimental setup and under the same conditions except for using only one particle species (with diameter  $4.38 \pm 0.06 \mu\text{m}$ , the total particle number in the field-of-view was  $N = 1945$ , resulting in higher density, thus higher nominal plasma frequency as in the bilayer case).

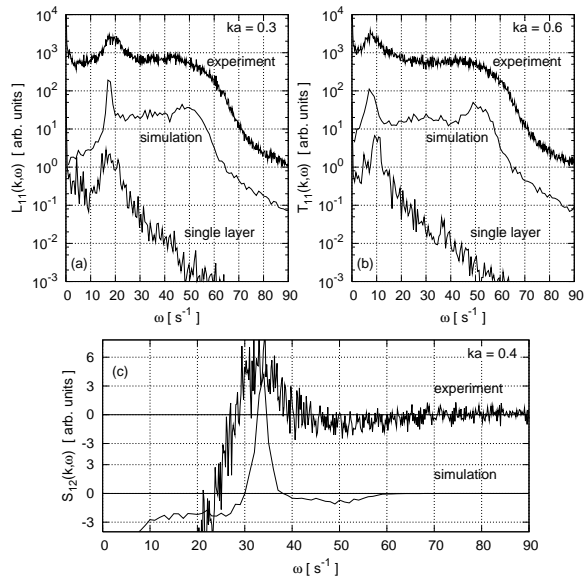


FIG. 2: Sample spectra illustrating the principal features of (a)  $L_{11}$  longitudinal, (b)  $T_{11}$  transverse current fluctuations and (c)  $S_{12}$  inter-layer density fluctuations. The one-layer spectra from the experiment and MD simulations are shown and compared to experimental single-layer spectra obtained in a separate measurement. The inter-layer spectra (experiment and MD simulation) show a positive and a negative peak representing the in-phase and out-of phase oscillations, respectively. The vertical scale is shifted for clarity.

In Fig. 2(a) and (b) one can observe both in the experiment and in the simulation the presence of a strong primary peak at lower frequencies and a shoulder-like, weak and wide feature at higher ( $\omega \approx 50 \text{s}^{-1}$ ) frequencies. The strength of this high-frequency peak becomes more obvious in comparison with the single layer situation, where at the same frequency the spectral power has already dropped two orders of magnitude, while it has the same slope as seen in the bilayer spectrum at higher frequencies ( $\omega > 70 \text{s}^{-1}$ ). Figure 2(c) shows the inter-layer density fluctuation spectrum  $S_{12}$  at  $ka = 0.4$  from the experiment and the MD simulation. The novel feature here is the appearance of a negative peak indicating an out-of-phase oscillation at the higher frequency, coinciding with the “shoulder” in the  $L_{11}$  and  $T_{11}$  spectra.

As it is expected, all spectral peaks are more pronounced and sharper in the simulation, where frictional damping and disturbing effect of the finite confinement are absent.

We compare our observational results with the mode dispersion calculated through two theoretical models. The first model is a perfect staggered rectangular lattice, with phonon propagation along the two principal axes. The lattice calculation is based on the formalism used in [7] for electronic bilayers, adopted to the asymmetric Yukawa system. The second model is a completely disordered solid bilayer, with the mode dispersion calculated in the Quasi-Localized Charge Approximation (QLCA) formalism. The QLCA formalism was adapted to the binary Yukawa bilayer system (based on [28, 29]) and the dispersions for the 4 modes were calculated with the input of the experimental pair-correlation functions. It should be noted that while for symmetric configurations the (in general)  $4 \times 4$  dynamical matrix can be decomposed into two  $2 \times 2$  matrices, resulting in a clear separation of the collective modes into longitudinal vs. transverse and in-phase vs. out-of-phase polarizations, in the present case, this kind of mode separation, in general, is not possible. It can be done only along the directions of the principal axes of the crystal, or in an approximation where the system is assumed to be isotropic as in the QLCA description.

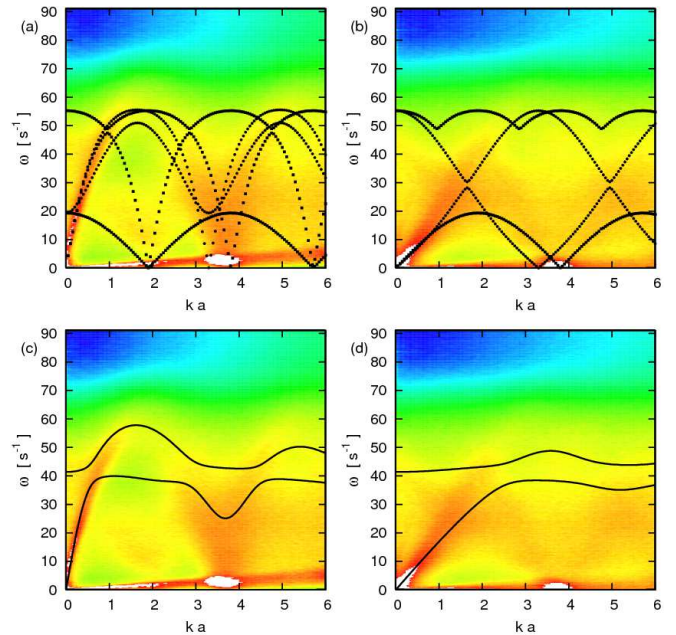


FIG. 3: (color online)  $L_{11}$  one-layer longitudinal (a,c) and  $T_{11}$  one-layer transverse (b,d) current fluctuation spectra. Peak positions (hot colors) mark the dispersion  $\omega(k)$ . Black symbols in (a,b) are frequencies from lattice summation calculations including the two principal lattice directions. Lines in (c,d) are the corresponding QLCA dispersions.

Figure 3 shows an example of the longitudinal and transverse current fluctuation spectra in the upper layer,

color coded in the wave-number ( $ka$ ) / frequency ( $\omega$ ) plane. Overlaid are a selected set of lattice dispersions (panels [a] and [b]), and the QLCA mode dispersions (panels [c] and [d]). An additional, very low frequency, linear dispersion can be seen, which is most likely the fingerprint of an unavoidable net motion of the ensemble.

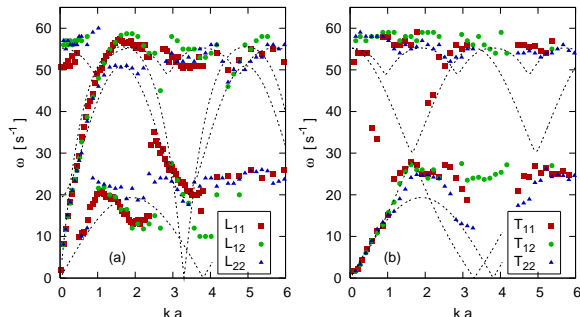


FIG. 4: (color online) Symbols: peaks identified in the longitudinal (a) and transverse (b) experimental spectra. Lines: selected lattice dispersions with  $x$  and  $y$  polarizations.

Figure 4 shows the more detailed dispersion properties of the dusty plasma bilayer together with lattice calculation results. The modes are not labeled, for reasons discussed above, only their sources (the spectra in which the peak was found) are indicated.

In Figs. 3 and 4 one can observe the expected acoustic modes similar to those in 2D Yukawa layers, and an optical excitation with finite and nearly constant frequency, even at very low wave-numbers. This latter mode is identified as the so called energy (frequency) gap, studied in great detail in earlier simulations and theoretically predicted through lattice calculations [7] and for strongly coupled liquids through the QLCA approach [8, 11]. The QLCA model provides the value of the gap frequency as

$$\omega_{\text{gap}}^2 = \frac{\omega_1^2}{2} \left( \frac{Z_2 n_2}{Z_1 n_1} + \frac{Z_2 m_1}{Z_1 m_2} \right) \int_0^\infty \mathcal{F}(r) g_{12}(r) dr, \quad (1)$$

where  $\omega_1^2 = (e^2 Z_1^2 n_1) / (2\varepsilon_0 m_1 \sqrt{a_1 a_2})$ , the kernel  $\mathcal{F}(r) = z^{-3} r e^{-w} [(1+w)(1-3d^2/z^2) + w^2]$ ,  $z = \sqrt{r^2 + d^2}$ , and  $w = z/\lambda_D$ .

In view of the prevailing local lattice structure in co-existence with a high degree of disorder it is not a priori clear, which of the two models (lattice vs. QLCA) should provide a better description of the mode structure. Inspection of Fig. 3 shows that for low  $k$  values the acoustic portions of the low frequency modes are equally well described by either model. For higher  $k$  values the repeated Brillouin zone structure is clearly visible, indicating the superiority of the lattice model. For the high frequency optic mode the QLCA predicts a single “frequency gap” at  $k = 0$  with Eq.(1):  $\omega_{\text{gap}}^{\text{exp}} = 41.4 \text{ s}^{-1}$  and  $\omega_{\text{gap}}^{\text{MD}} = 43.5 \text{ s}^{-1}$  calculated with the input of experimental and simulation  $g_{12}(r)$  data. This value and the high- $k$

tapering off of the optic modes seem to be more along the line of the QLCA description.

We can conclude, that our dusty plasma experiment using two different dust sizes created a strongly coupled bilayer system that can be well approximated by a unipolar binary Yukawa bilayer model. This model has served as the basis for MD simulations, lattice calculations, and a QLCA calculation. All these approaches are in good agreement with the experiment, and verify the presence of an optical collective mode characterized by a finite energy (frequency) gap at  $k = 0$  wave-number, distinguishing the strongly coupled bilayer from a weakly coupled one, where all the modes have an acoustic character.

Work partially supported by NSF Grants PHY-0813153, PHY-0812956, DOE Grants DE-FG02-03ER54716, DE-FG02-04ER54804 and OTKA-K-77653, OTKA-PD-75113, MTA-NSF/102. This paper was supported by the Janos Bolyai Research Scholarship of the Hungarian Academy of Sciences. Experimental setup was partially donated by the MOM-Szerviz Kft, and assembled by J. Forgács, J. Tóth, and Gy. Császár.

- 
- [1] J. A. Seamons *et al.*, *Phys. Rev. Lett.* **102**, 026804 (2009).
  - [2] T. B. Mitchell *et al.*, *Science* **282**, 1290 (1998).
  - [3] E. B. Watkins *et al.*, *Phys. Rev. Lett.* **102**, 238101 (2009).
  - [4] O. I. Yuzepovich *et al.*, *Low Temp. Phys.* **34**, 985 (2008).
  - [5] S. Das Sarma and A. Madhukar, *Phys. Rev. B* **23**, 805 (1981); for more references, see those in Ref. [8](c)
  - [6] Yu. M. Vil'k and Yu. P. Monarkha, *Soviet Journal of Low Temperature Physics* **11**, 535 (1985).
  - [7] G. Goldoni and F. M. Peeters, *Phys. Rev. B* **53**, 4591 (1996).
  - [8] (a) K. I. Golden and G. Kalman, *Phys. Stat. Sol. B* **180**, 533 (1993); (b) G. J. Kalman, Y. Ren, and K. I. Golden, *Phys. Rev. B* **50**, 2031 (1994); (c) G. J. Kalman, V. Valtchinov, and K. I. Golden, *Phys. Rev. Lett.* **82**, 3124 (1999).
  - [9] I. V. Schweigert *et al.*, *Phys. Rev. Lett.* **82**, 5293 (1999).
  - [10] Z. Donkó and G. J. Kalman, *Phys. Rev. E* **63**, 061504 (2001).
  - [11] Z. Donkó *et al.*, *Phys. Rev. Lett.* **90**, 226804 (2003); Z. Donkó *et al.*, *J. Phys. A: Math. Gen.* **36** 5877 (2003).
  - [12] R. Messina and H. Löwen, *Phys. Rev. Lett.* **91**, 146101 (2003).
  - [13] S. Ranganathan and R. E. Johnson, *Phys. Rev. B* **69**, 085310 (2004).
  - [14] P. Hartmann *et al.*, *Europhys. Lett.* **72**, 396 (2005).
  - [15] G. J. Kalman *et al.*, *Phys. Rev. Lett.* **98**, 236801 (2007).
  - [16] S. Ranganathan and R. E. Johnson, *Phys. Rev. B* **75**, 155314 (2007).
  - [17] A. Filinov *et al.*, *J. Phys.: Conf. Ser.* **35**, 197 (2006).
  - [18] S. De Palo *et al.*, *Phys. Rev Lett.* **88**, 206401 (2002).
  - [19] G. E. Astrakharchik, J. Boronat, I. L. Kurbakov, and Yu. E. Lozovik, *Phys. Rev. Lett.* **98**, 060405 (2007).
  - [20] B. Smith, T. Hyde, L. Matthews, J. Reay, M. Cook, and J. Schmoke, *Advances in Space Research* **41**, 1509 (2008).
  - [21] L. S. Matthews, K. Qiao, T. W. Hyde, *Advances in Space*

- Research* **38**, 2564 (2006).
- [22] S. Ranganathan and R. E. Johnson, *Phys. Rev. B* **78**, 195323 (2008).
- [23] D. S. Kainth *et al.*, *J. Phys. Cond. Matter* **12**, 439 (2000).
- [24] Y. Feng *et al.*, *Rev. Sci. Instr.* **78**, 053704 (2007).
- [25] G.J. Kalman *et al.*, *Condensed Matter Theories* **13**, 203 (1997).
- [26] M. Lampe *et al.*, *Phys. Plasmas* **7**, 3851 (2000).
- [27] J. P. Hansen *et al.*, *Phys. Rev. A* **11**, 1025 (1975).
- [28] K.I. Golden and G.J. Kalman, *Phys. Plasmas* **7**, 14 (2000).
- [29] Z. Donkó *et al.*, *Book of Abstracts*, 12th Workshop on the Physics of Dusty Plasmas, Boulder, Colorado, USA, May 17 - 20, (2009).